Proceedings of the ASME 2025 International Design Engineering Technical Conferences & Computers and Information in Engineering Conference
IDETC/CIE 2025
August 17-20, 2025, Anaheim, CA, USA

IDETC/CIE 2025-169092

ELECTRIC VEHICLE CHARGING NETWORK OPTIMIZATION CONSIDERING REGIONAL RESOURCE DEPENDENCIES

Yinshuang Xiao
Walker Dept. of Mechanical Engineering
The University of Texas at Austin
Austin, Texas 78712-1591
Email: yinshuangxiao@utexas.edu

Harshal D. Kaushik
Dept. of Mechanical Engineering
The University of Texas at Dallas
Richardson, Texas 75080
Email: Harshal.Kaushik@utdallas.edu

Jingbo Wang
Dept. of Mechanical Engineering
The University of Texas at Dallas
Richardson, Texas 75080
Email: Jingbo.Wang@utdallas.edu

Jie Zhang
Dept. of Mechanical Engineering
The University of Texas at Dallas
Richardson, Texas 75080
Email: jiezhang@utdallas.edu

Zhenghui Sha*
Walker Dept. of Mechanical Engineering
The University of Texas at Austin
Austin, Texas 78712-1591
Email: zsha@austin.utexas.edu

ABSTRACT

The optimal allocation of electric vehicle (EV) charging resources is crucial for advancing national electrification and decarbonization plans, prompting extensive research into efficient placement strategies for EV charging infrastructure. While many aim to maximize the coverage of charging resources based on demand, typical approaches adopt uniform grid cells to divide the region of interest for analysis. However, these methods often overlook spillover effects (i.e., dependencies) between sub-regions, where high charging demand in one sub-region spreads to surrounding areas. To address this limitation, we develop a novel bipartite network-based design decision-making framework for optimal placement and allocation of EV charging stations, including the number and type of chargers. The proposed framework introduces two key innovations. First, it includes a new partition method integrating Voronoi diagrams with K-means clustering to mitigate the spillover effects inherent in grid-based methods. This method aggregates charging demand by accounting for points of interest (POIs) and traffic flow through K-means clustering and then partitions the region of interest into Voronoi cells based on the clustered centroids. Second, the framework adopts the choice modeling philosophy and uses a bipartite network model to represent "customer" nodes (i.e., EV drivers in a service zone defined by a Voronoi cell) and "product" nodes (i.e., charging stations). A link is established between a station and its corresponding service zone if it lies within the zone. For service zones without a station, links are created to the nearest station based on the shortest driving distance calculated from the real-world transportation network, incorporating driving costs. With such a choice modeling method, the charging demand can be explicitly represented to support optimal resource allocation, including the location of stations and the number and type of chargers. To demonstrate and validate the proposed framework, we formulate an optimization problem to maximize the coverage of public EV charging resources in Austin, Texas, while minimizing the driving cost and total expenses, subject to budget and power grid constraints.

Keywords: Electric vehicles, resource allocation, bipartite network, Voronoi-K-means partitioning.

*Corresponding author.

1 INTRODUCTION

The global transition from conventional automobiles to electric vehicles (EVs) is a critical strategy for achieving the climate goal of net-zero emissions by 2050 [1]. This shift is evident in the concerted efforts of governments and industries worldwide. In 2022, plug-in EVs accounted for 14% of the global light-duty vehicle market, with China and Europe leading at 29% and 21%, respectively [2]. By 2024, plug-in EVs constituted 9.9% of all passenger vehicle sales, and over 6.4 million plug-in EVs had been sold in the U.S. by January 2025 [3]. Projections suggest that new policies and industry targets could increase the market share of plug-in EVs to between 48% and 61% of the U.S. light-duty vehicle sector by 2030 [2].

To support this growth, the *2030 National Charging Network report* estimates that the U.S. will require 182,000 DC fast chargers (each with a minimum capacity of 150 kW) and 1,067,000 Level 2 public chargers by 2030, based on a projected 33 million EVs on the road [2]. This infrastructure expansion is expected to necessitate a cumulative capital investment of 31–55 billion USD in publicly accessible charging infrastructure. As of now, data from the Station Locator indicates that only 13.3% of the required DC fast chargers and 13.4% of the necessary Level 2 charging stations are operational, highlighting the significant gap that remains to be addressed [4].

Planning for EV charging infrastructure is critical to alleviating range anxiety among EV drivers and promoting widespread adoption of EVs. However, the efficient deployment of such infrastructure is influenced by numerous factors, including user demand and charging behaviors [5, 6], location and accessibility [7], cost and funding considerations [8, 9], grid capacity and stability [10], available charging technologies (e.g., charger types) [11], and regulatory policies governing installation, maintenance, and operation [12]. To address the significant gap between charging resource demand and supply, and to better understand how these factors influence infrastructure planning, extensive research has been conducted. For instance, Wang et al. proposed a heterogeneous spatial-temporal graph convolutional network for short-term EV charging demand prediction, leveraging point-of-interest (POI) data to design a region-specific prediction module [6]. Their model was validated using real-world GPS trajectory data. In another work, Nicholas provided detailed estimates of capital costs for EV charging infrastructure across 100 major U.S. metropolitan areas, underscoring the need for substantial investment to support EV growth while identifying gaps in cost estimates, such as fast-charging corridors and project management [9]. Additionally, Acharige et al. conducted a comprehensive review of EV charging technologies, international standards, charging station architectures, and power converter configurations [11].

To further synthesize existing research, we examined several recent review articles that approach EV charging infrastructure planning from diverse perspectives. For example, Anadon and Sumper focused on public EV charging infrastructure planning, organizing the literature around the perspectives and objectives of key stakeholders in the EV charging value chain, including EV users, charging operators, service providers, and power system infrastructure [13]. In another study, Ullah et al. categorized optimal charging station placement approaches into five methodologies: 1) flow-based approaches, which optimize resource allocation for intercity stations by managing electricity, information, and payment flows; 2) node-based approaches, which divide networks into nodes for real-time monitoring, suitable for intracity stations; 3) path-based approaches, which optimize charging along planned vehicle routes to ensure accessibility without overloading infrastructure; 4) tour-based approaches, which create itineraries with charging stops for random or round trips; and 5) network equilibrium approaches, which balance supply and demand by integrating power and transport networks for optimal station placement [14].

Building on the insights from the literature review, it is evident that optimal EV charging infrastructure planning requires dual foci: accurate regional charging demand prediction and optimal placement and allocation of charging resources. An ideal framework would integrate these two aspects while accounting for key influencing factors such as user behavior, grid capacity, cost constraints, and regulatory policies. However, despite significant advances in the field, a critical limitation is that existing approaches rely on uniform grid-based methods to partition regions of interest for analysis [5, 6, 15]. While these methods provide a structured approach, they overlook the interdependencies between sub-regions, such as the spillover effects, where high charging demand in one area can significantly influence adjacent regions. This limitation results in suboptimal resource allocation. Consequently, current methods fail to provide a holistic solution that addresses the interconnected nature of EV charging demand, hindering the development of efficient and scalable charging networks.

To address these challenges, we propose a novel bipartite network-based framework for optimal placement and allocation of EV charging stations, including the determination of charger types and quantities. Our framework overcomes the limitations of traditional grid-based methods and has two key innovations. First, we introduce a new partition method that integrates Voronoi diagrams [16] with weighted K-means clustering [17]. Unlike uniform grid-based approaches, this method accounts for the varying influence of spatially relevant factors, such as points of interest (POIs) and traffic flow patterns, on charging behaviors. By weighting these factors, the method aggregates the charging demand through weighted K-means clustering. The resulting clusters are used to generate Voronoi cells, which partition the region into service zones that more accurately reflect real-world demand distribution and mitigate spillover effects between sub-regions. As a result, this approach enables better capture of spatial heterogeneity in charging demand, thus enabling a more

efficient resource allocation.

Second, our framework adopts a choice modeling philosophy [18, 19], leveraging a bipartite network structure to model the interactions between EV drivers and charging stations. In this network, "customer" nodes represent EV drivers within a service zone defined by a Voronoi cell, while "product" nodes represent charging stations. Links are established between stations and their corresponding service zones if they are located within the zone. For service zones without a station, links are created to the nearest station based on the shortest driving distance derived from the real-world transportation network, incorporating considerations of driving costs. This bipartite network representation not only explicitly captures charging demand but also accounts for resource dependencies between sub-regions, thus providing a more holistic solution to efficient and equitable infrastructure planning. To validate the applicability of our proposed framework, we conduct a case study on public charging stations in Austin, Texas, formulating an optimization problem that maximizes the coverage of EV charging resources while minimizing total expenses and driving cost, subject to budget and power grid constraints.

The remainder of the paper is organized as follows. Section 2 introduces the proposed bipartite network-based framework for EV charging station planning. Section 3 presents the details of the case study. Section 4 discusses the limitations of this work. Finally, Section 5 concludes the paper with closing remarks and outlines potential directions for future research.

2 RESEARCH FRAMEWORK

Figure 1 provides an overview of the bipartite network-based design decision-making framework for the optimal placement and allocation of EV charging stations. The framework consists of three key steps: 1) partitioning the region of interest into local service zones with similar charging demand, 2) representing the charging demand-supply relationship as a bipartite network, and 3) formulating an optimization problem to optimize the design of the EV charging system. The following subsections elaborate on each step in detail.

2.1 STEP 1: CHARGING DEMAND PARTITION

In Step 1, our objective is to partition the region of interest into local service zones, with each zone having similar charging demand. This step is critical to efficiently allocate local charging demands to charging resources (stations), thus optimizing the operation of the entire charging system. In addition, this process identifies candidate locations for the establishment of new stations. To achieve this, we propose a partitioning method that integrates Voronoi diagrams and K-means clustering. Figure 2 illustrates the flowchart of the proposed method using a toy example. The flowchart consists of two major parts. The first part, represented by the upper row of the flowchart, identifies the impact of different featured locations on charging demand. In this example, we first apply K-means clustering to group locations, including existing EV charging stations and two types of point-of-interests (POIs), such as cafes and theaters, based solely on their geographic coordinates. Locations with closer distances are grouped into clusters, and the centroids of these clusters are identified [20]. These centroids are then used as seed points to partition the region using a Voronoi diagram. By definition, a Voronoi cell consists of all points in the region that are closer to its seed point than any other seed point [16]. In the context of EV charging, stations within a Voronoi cell naturally serve EV drivers visiting POIs within the same zone, assuming distance is the primary consideration. However, existing studies have shown that different POIs and local traffic flow have varying levels of influence on charging demand [21, 22]. To account for this, we formulate a regression model to analyze and rank the importance of these factors.

In the regression model, the dependent variable is the number of EVs charged in each service zone over a specific period (e.g., a day or week). The independent variables include the number of charging stations, different POIs, and traffic flow (e.g., the number of cars captured by traffic cameras, if data is available) within each service zone. To ensure comparability, all independent variables are normalized. The regression model estimates the coefficients for each factor, allowing us to rank their contributions to charging demand. Factors with higher contributions are assigned larger weights, reflecting their relative importance.

Once the weights are determined for the different featured locations, we proceed to the second part of the flowchart, corresponding to the bottom row of Figure 2. In this part, we update the Voronoi partition by incorporating these weights. For instance, in the toy example, assuming the regression model assigns weights of 3, 2, and 1 to EV charging stations, theaters, and cafes, respectively. We then apply weighted K-means clustering to regroup the locations and recalculate the centroids based on these weights. Using the updated centroids as seed points, we re-partition the region. Returning to the toy example, the new centroid of the upper-left service zone is "dragged" closer to the charging station due to its higher weight compared to the cafe. Consequently, the boundary of the service zone is adjusted accordingly. Through regression analysis and weighted clustering, the method partitions the region into service zones with similar charging demand. Zones in denser, high-demand areas are smaller and more granular, while lower-demand areas will be partitioned into larger zones. By incorporating the influence of key factors such as POIs and traffic flow, the weighted clustering ensures that each zone accurately reflects the characteristics of local demand. This approach goes beyond geographic proximity, creating service zones more aligned with underlying charging demand patterns.

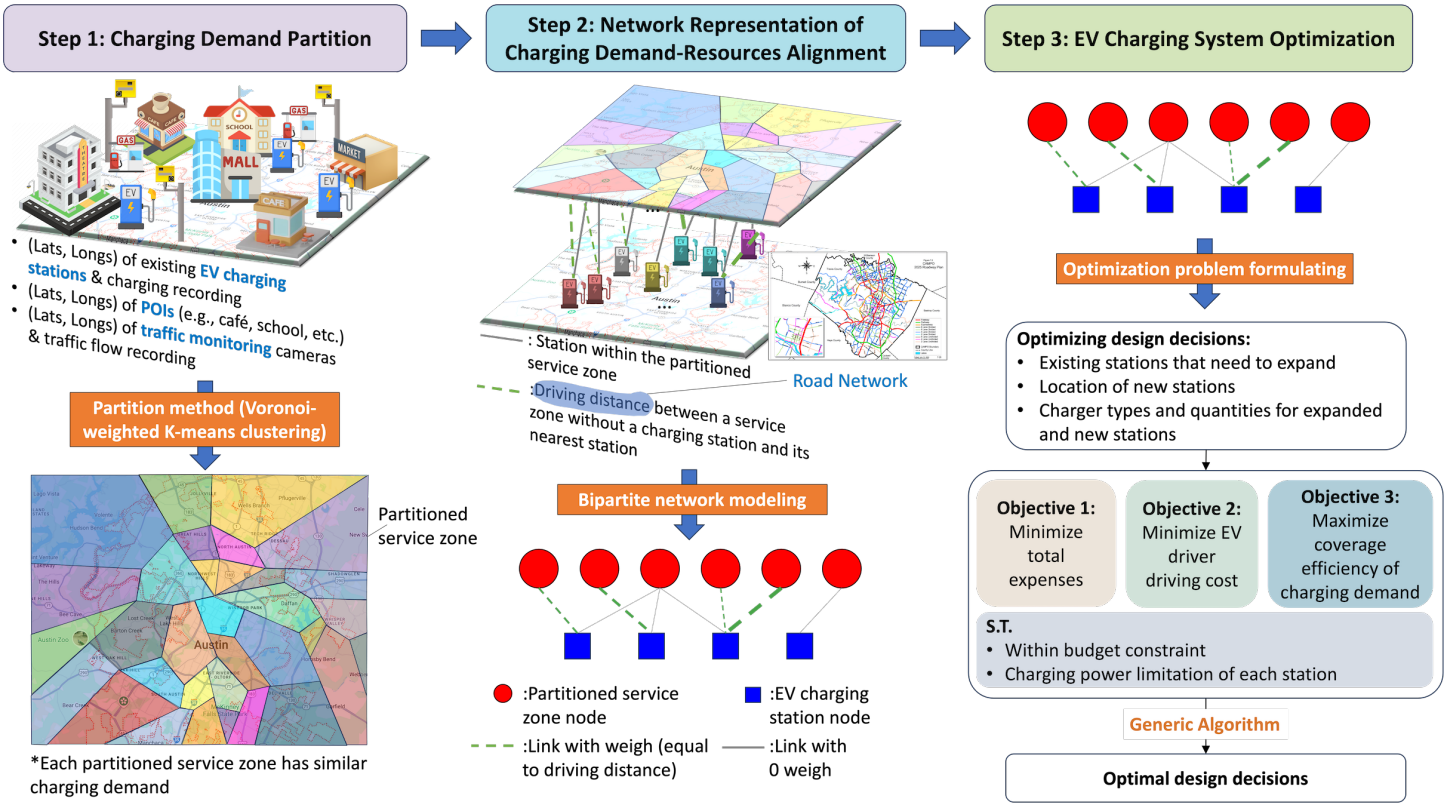

FIGURE 1: Bipartite network-based design decision-making framework for the optimal placement and allocation of EV charging stations. Note that this framework highlights the key components of each step; detailed illustrations are provided in the corresponding sections.

FIGURE 2: Flowchart of the geographical partitioning method for charging demand.

2.2 STEP 2: NETWORK REPRESENTATION OF CHARGING DEMAND-RESOURCES ALIGNMENT

In this step, we construct a bipartite network to represent charging demand and resources. As outlined in Algorithm 1, the process involves two critical sub-steps. First, we define two types of nodes. Node type "A" represents the centroids of partitioned service zones, with geographic coordinates and service zone IDs as node attributes. These centroids, representing localized aggregations of charging demand, are treated as "customers" in accordance with choice modeling principles. Node type "B" represents existing EV charging stations, with geographic coordinates as node attributes. These stations, which provide charging services, are treated as "products" in the choice model.

The second sub-step involves constructing links based on two key assumptions. The first assumption is that if a charging station is located within a service zone, it is considered the natural choice for EV drivers within that zone to charge their vehicles. Consequently, we generate a link between the station and the centroid of the service zone, assigning it a driving effort of zero (i.e., link weight = 0). The second assumption is that if a service zone does not have any charging stations, EV drivers within that zone will seek charging resources from nearby stations. Therefore, we generate links between the centroid of the zone and the top k nearest stations, with the link weight equal to the driving distance. These nearest stations and shortest driving distances are identified and calculated using Dijkstra's algorithm [23], based on the real-world road network. This approach ensures a realistic representation of the charging behavior and resource allocation.

2.3 STEP 3: EV CHARGING SYSTEM OPTIMIZATION

In Step 3, we formulate an optimization problem to optimize the placement and allocation of EV charging stations based on the bipartite network model. As illustrated in Figure 1, three types of design decisions are considered: 1) identifying which existing stations require expansion, 2) selecting appropriate locations from a set S_{new} of potential new charging stations (derived from centroid locations of service zones without stations), and 3) determining charger types and quantities for both expanded and new stations. The optimization objectives include minimizing total expenses, minimizing total driving costs, and maximizing the coverage of charging demand. Additionally, two constraints are imposed: 1) the total expenses must remain within a given budget, and 2) the design decisions must adhere to power limitations to prevent overloading the connected power grid. For simplification, in this work, we assign a fixed power limitation value to each station. However, our future work aims to incorporate the real power grid structure to ensure that the expanded and new stations comply with the power limitations at their connection points. Next, we provide further details on the formulation of the three objectives and the solution process for the optimization problem.

Algorithm 1 Build Bipartite Graph

Input: Polygon set O, centroid set U for partitioned service zones, existing EV charging station set S, road network G, and integer k
Output: Bipartite graph H

$H \leftarrow$ new graph()
▷ Add nodes
for each *idx* in U **do**
  H.add_node(("A", *idx*), coordinate=(*lat*, *lon*), poly_id=$V[idx]$)
end for
for each *idx* in S **do**
  H.add_node(("B", *idx*), coordinate=(*lat*, *lon*))
end for
▷ Construct edges
for each *A_idx* in H.nodes["A"] **do**
  poly_idx=*A_idx*["poly_id"]
  poly=$O[poly\_idx]$
  sub_s=[H.nodes["B"]["coordinate"] in *poly*]
  if *sub_s* $\neq$ None **then**
    for each *B_idx* in *sub_s* **do**
      H.add_edge(*A_idx*, *B_idx*, distance=0)
    end for
  else
    Dist = {}
    for each *B_idx* in H.nodes["B"] **do**
      dist = Caculate_Driving_Distance(G, H.nodes[*A_idx*], H.nodes[*B_idx*])
      Dist["*B_idx*"]=*dist*
    end for
    sorted_Dist=sorted(*Dist*, key=lambda *x*: *x*[1], reverse=False)
    $top\_k\_dist = sorted\_Dist[:k]$
    for *b_idx*,*val* in top_k_dist **do**
      H.add_edge(*A_idx*, *b_idx*, distance=*val*)
    end for
  end if
end for
return H

2.4 TOTAL EXPENSES

In this work, we focus primarily on public charging stations. Following [9], the installation costs for chargers include hardware costs and associated expenses such as labor, materials, permits, and taxes, which vary with the number of chargers installed. For example, the costs of installing q_1 number of Level 2 chargers with 6.6 kW[1] and q_2 number of DC 50 kW chargers in public

[1] This is the price outside California.

and workplace stations are provided in Equation (1) and Equation (2), respectively,

$$c_{Level2} = \begin{cases} (3127+2836)q_1 & \text{if } q_1 = 1 \\ (3127+3020)q_1 & \text{if } q_1 = 2 \\ (3127+3090)q_1 & \text{if } 3 \le q_1 \le 5 \\ (3127+2305)q_1 & \text{if } 6 \le q_1 \le 100, \end{cases} \tag{1}$$

$$c_{DC50} = \begin{cases} (28401+45506)q_2 & \text{if } q_2 = 1 \\ (28401+36235)q_2 & \text{if } q_2 = 2 \\ (28401+26964)q_2 & \text{if } 3 \le q_2 \le 5 \\ (28401+17692)q_2 & \text{if } 6 \le q_2 \le 50. \end{cases} \tag{2}$$

These costs are reported in 2019, with future costs assumed to decline at a rate of 3% annually. Assuming we consider only Level 2 and DC 50 kW chargers and do not differentiate between station expansion and new station establishment (i.e., the cost of installing two Level 2 chargers is the same for both scenarios), the total expenses can be calculated using Equation (3),

$$C = \left(\sum_{i \in S} C_i + \sum_{j \in S_{new}} C_j \right) (1 - 3\%(Year - 2019)). \tag{3}$$

As previously mentioned, S represents the set of existing EV charging stations, and S_{new} denotes the set of candidate centroids of those service zones without EV charging stations and are ready for establishing new stations. The expense of expanding an existing station i is given by $C_i = c_{Level2}(q_1^i) + c_{DC50}(q_2^i)$, where q_1^i and q_2^i are the number of Level 2 and DC 50 kW chargers added to station i, respectively. Similarly, C_j is the expense of establishing a new station j, and $C_j = c_{Level2}(q_1^j) + c_{DC50}(q_2^j)$, where q_1^j and q_2^j represent the number of Level 2 and DC 50 kW chargers installed at station j. For a station in S or S_{new}, if both q_1 and q_2 are zero, this indicates that the existing station will not be expanded or the candidate station will not be built. The variable $Year$ corresponds to a future year of interest after 2019. Equation (3) defines our first objective function, which aims to minimize the total cost C by optimizing the integer variables q_1^i, q_2^i, q_1^j, and q_2^j.

2.5 DRIVING COST AND COVERAGE EFFICIENCY OF CHARGING DEMAND

Figure 3 presents an illustrative example to demonstrate the calculation of driving costs and coverage efficiency. The

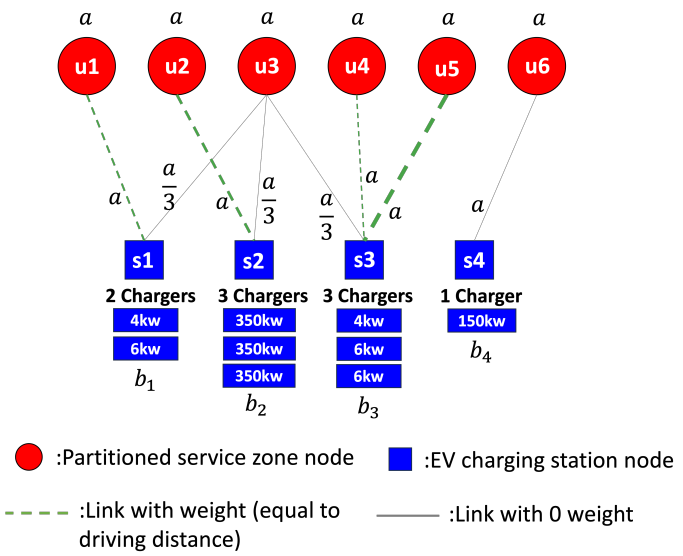

FIGURE 3: A toy example to illustrate the calculation of driving cost and coverage efficiency.

bipartite network generated by Algorithm 1 is represented as $H = (U, S, E, W)$, where U and S denote the sets of service zone nodes and charging station nodes, respectively. E is the set of links and W stores the corresponding link weights. We assume a represents the charging demand (the approximate number of EVs requiring charging within a specific period, e.g., a day or week) for each service zone, and b_i represents the charging capacity of station s_i (the approximate total number of EVs charged during the same period) determined by the type and number of chargers it hosts. For each service zone node u_j, its charging demand is evenly divided by its degree $\deg(u_j)$ and assigned to the connected stations. For example, in Figure 3, the degree of service zone u_3 is 3, so its charging demand is divided into three equal parts, $\frac{a}{3}$, and assigned to stations s_1, s_2, and s_3. The total assigned charging demand for any station s_i is calculated as:

$$\text{assignedDemand}(s_i) = \sum_{u_j:(u_j,s_i)\in E} \frac{a}{\deg(u_j)}. \tag{4}$$

If $\text{assignedDemand}(s_i) \le b_i$, station s_i covers all assigned demand. Otherwise, it covers only a fraction of the demand from each link (u_j, s_i), proportional to $\frac{b_i}{\text{assignedDemand}(s_i)}$. Thus, the demand covered through link (u_j, s_i) is:

$$\text{covered}_{u_j,s_i} = \frac{a}{\deg(u_j)} \times \frac{b_i}{\text{assignedDemand}(s_i)}. \tag{5}$$

The total driving cost is then calculated as:

$$D = \sum_{(u_j,s_i)} \text{covered}_{u_j,s_i} \cdot w_{u_j,s_i}, \tag{6}$$

where w_{u_j,s_i} is the weight of link (u_j, s_i), representing the driving distance between zone u_j and station s_i. This equation reflects the total driving distance for all $\text{covered}_{u_j,s_i}$ EVs transferring through link (u_j, s_i). Next, regarding the coverage efficiency, the total covered demand for all zones in U is:

$$\text{COVERED} = \sum_{u_j \in U} \sum_{s_i:(u_j,s_i)\in E} \text{covered}_{u_j,s_i}. \tag{7}$$

The total unmet demand is calculated as:

$$Q = \sum_{u_j \in U} \sum_{s_i:(u_j,s_i)\in E} (a - \text{covered}_{u_j,s_i}). \tag{8}$$

Equations (6) and (8) define our second and third objective functions, aiming to minimize the total driving cost D and unmet charging demand Q, respectively. Since both D and Q depend on the structure of network H, their minimization is directly influenced by the number of Level 2 and DC 50 kW chargers expanded at existing stations or installed at new stations.

2.6 BUDGET AND POWER CONSTRAINTS

In this work, we incorporate two constraints. The first constraint is the budget C_{budget}. We penalize any total cost exceeding the budget, defined as:

$$C_{penalty} = \begin{cases} 0 & \text{if } C \le C_{budget} \\ C - C_{budget} & \text{if } C > C_{budget}. \end{cases} \tag{9}$$

The second constraint relates to the power limitation of each station. According to [9], a typical station has a site power limit of $P_{threshold} = 2.5$ megawatts of power. To ensure compliance with this constraint, we penalize any power usage exceeding the threshold for each station, and the penalty is defined as:

$$P_{penalty} = \sum_{s_i \in S} (P_{s_i} - P_{threshold}). \tag{10}$$

where P_{s_i} is the total power supported by the station s_i, and it is a function of the design variables q_1, q_2 as below:

$$P_{s_i} = \begin{cases} P^i_{ext} + 6.6q_1 + 50q_2 & s_i \text{ is existing station} \\ 6.6q_1 + 50q_2 & s_i \text{ is new station} \end{cases} \tag{11}$$

where P^i_{ext} represents the total power already available at the existing station s_i, which can be determined from existing data.

2.7 SOLVING THE OPTIMIZATION PROBLEM

In this work, the computation of driving costs and coverage efficiency relies heavily on the developed bipartite network models. Consequently, the search for an optimal solution is conducted using metaheuristic approaches. Specifically, we employ a genetic algorithm (GA) [24] to solve the optimization problem. As outlined in Algorithm 3, the hyperparameters include "popSize", which defines the population size in each iteration; "maxiter", which specifies the maximum number of generations for the GA search; and "run", which determines the maximum number of consecutive generations without improvement in the best objective value (fitness), triggering the termination of the search. The design variable vector Q is a 1D integer vector encoding the number of Level 2 and DC 50 kW chargers installed across all existing stations (total M) and candidate stations (total N). It is formatted as $[q_1^1, q_2^1, ..., q_1^M, q_2^M, q_1^{M+1}, q_2^{M+1}, ..., q_1^{M+N}, q_2^{M+N}]$, where q_1^{max} and q_2^{max} represent the predefined maximum number of Level 2 and DC 50 kW chargers allowed per station, respectively. The fitness function, which depends on $\mathbf{Q}$, is computed using Algorithm 2. Within this algorithm, the three objective functions, C, D, and Q, are normalized using max-min normalization to ensure that they operate on similar scales, thus avoiding bias toward any single objective, but can be adjusted based on needs. In contrast, the penalty terms $C_{penalty}$ and $P_{penalty}$ are retained at their original scales to impose significant penalties for violating budget and power constraints, ensuring that solutions adhere to these critical limitations.

3 CASE STUDY

In this section, we present a case study of public EV charging stations in Austin, Texas, to demonstrate the research framework introduced in Section 2.

3.1 DATA SOURCE

Multiple datasets were used to support the analysis and calculations in this study. These datasets were preprocessed to ensure they fall within the region of our interest, i.e., city Austin defined by the geographical boundaries: [min_lat, max_lat]

Algorithm 2 Fitness Function

Input: Design variable vector $\mathbf{Q}$, polygon set O, centroid set U for partitioned service zones, existing EV charging station set S, road network G, and integer k

Output: Fitness value $Val_{fitness}$

1: Given $\mathbf{Q}$, calculate C, $C_{penalty}$ and $P_{penalty}$
2: Given $\mathbf{Q}$, call Algorithm 1 to get the structure of network H
3: Given $\mathbf{Q}$ and H, calculate D and Q
4: Normalize C, D, and Q to get C_{norm}, D_{norm}, and Q_{norm}
5: $Val_{fitness} = C_{norm} + D_{norm} + Q_{norm} + C_{penalty} + P_{penalty}$
6: **return** $Val_{fitness}$

Algorithm 3 Optimal EV Charging Infrastructure Planning

Input: Polygon set O, centroid set U for partitioned service zones, existing EV charging station set S, road network G, and integer k

Output: Optimal solution for design variable vector $\mathbf{Q}$

1: GA (type = integer,
2: fitness($\mathbf{Q}$),
3: max = $[q_1^{max}, q_2^{max}]$,
4: popSize, maxiter, run)
5: **return** Solution of $\mathbf{Q}$

= [30.0255, 30.6376] and [min_lon, max_lon] = [-98.1821, -97.3755]. Table 1 summarizes the preprocessed data, while Figure 4 illustrates the geographical distribution of EV charging stations, POIs, and traffic cameras in the Austin area.

3.2 CHARGE DEMAND PARTITION

Following the proposed framework, we first partition the region based on the geo-locations of all EV charging stations, six types of POIs, and traffic cameras. The number of service zones is set to 200. The resulting partition is shown in Figure 5a. Next, we conduct regression analysis to assess the contributions of different location types to charging demand. In this case study, the dependent variable is the daily number of EVs charged at stations within each service zone, representing local charging demand. The independent variables include the number of different POIs and the average traffic flow in each zone. Notably, the number of existing EV charging stations in a zone exhibits a high correlation with charging demand (> 0.8), and so does the number of theaters (> 0.7). To avoid multicollinearity, we rank existing EV charging stations as the top contributor to local charging demand. The regression results for the remaining factors are provided in Table 2.

The coefficient estimates suggest that theater has a strong positive relationship with EV charging demand (coefficient = 503.53, $p = 0.001$). Shopping malls also show a statistically significant positive effect (coefficient = 266.40, $p = 0.018$), though

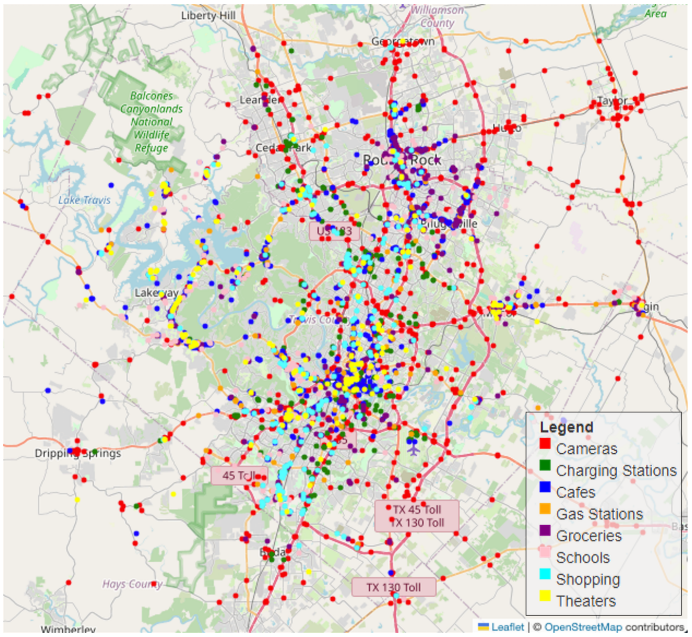

FIGURE 4: Geographical distribution of EV charging stations, POIs, and traffic cameras in Austin, Texas areas.

slightly smaller in magnitude. Meanwhile, gas stations exhibit a negative coefficient (-289.36) that is close to traditional significance ($p = 0.061$). Other variables, such as traffic flow, cafes, schools, and groceries, are not statistically significant. Based on these findings, we rank and weight the featured locations as shown in Table 3. Specifically: 1) EV charging stations are ranked as the top correlated factor; 2) theaters and shopping malls, which have significant positive effects, are ranked second and third, respectively; 3) gas stations, despite their negative impact, are ranked last; 4) factors with negligible effects are equally ranked between shopping malls and gas stations.

Based on the weights provided in Table 3, we repartitioned the study region into 200 new service zones, as shown in Figure 5b. In Figure 5a, the centroids are more uniformly distributed, resulting in relatively evenly sized local service zones across the region. In contrast, Figure 5b shows a higher concentration of centroids, representing aggregated charging demands, in the central urban area, with fewer centroids in peripheral regions. This indicates that smaller partitioned service zones in the city center can accommodate comparable charging demand to larger service zones in outlying areas. This pattern reflects the influence of high-impact factors, such as theaters and shopping malls, which are more densely located in urban cores, leading to a demand-driven allocation of service zones. Again, the results highlight the importance of incorporating weighted factors into partitioning methods to better align infrastructure planning with spatial variations in charging demand.

TABLE 1: Summary of datasets used in the case study

Dataset Name	Format	Size	Attribute being Used	Source of Data
Public EV charging stations	Tabular	398 stations	Latitude, longitude, # of available chargers and their powers # of EVs charged in a day	Google Maps
POIs	Tabular	1069 cafes, 295 gas stations, 467 groceries, 225 schools, 379 shopping malls, 254 theaters	Latitude, longitude	Google Maps
Traffic flow	Tabular	922 traffic camera locations	Latitude, longitude, # of cars recorded by camera	Texas Department of Transportation
Austin EV registration data	Tabular	280,686 EVs across 2017 to 2024	ZIP code, registration date	Atlas EV Hub[1]
Austin roadway network	Line Shapefiles	-	-	Texas Department of Transportation

[1] Atlas EV Hub Link

TABLE 2: Regression results: the impact of traffic flow, POIs on EV charging demand[1]

	Coef	Std err	t	$p > \|t\|$
Const	20.4080	40.253	0.507	0.614
Avg traffic flow	129.3872	117.843	1.098	0.275
Cafe	165.8253	139.349	1.190	0.237
School	0.6702	148.991	0.004	0.996
Theater	503.5305	149.573	3.366	0.001
Gas station	-289.3638	152.465	-1.898	0.061
Shopping mall	266.3993	110.148	2.419	0.018
Grocery	41.1328	156.131	0.263	0.793

[1] All data used to estimate this regression model is normalized using min-max normalization.

TABLE 3: Ranking and weighting impacts of different featured locations in charging demand

Featured locations	Rank	Weight
EV charging station	1	5
Theater	2	4
Shopping mall	3	3
Theater	4	2
Avg traffic flow	4	2
Grocery	4	2
School	4	2
Gas station	5	1

3.3 BIPARTITE NETWORK MODELING

After partitioning the service zones, we input the polygon and centroid sets of the 200 service zones, along with the set of 398 existing public EV charging stations, into Algorithm 1 to simulate the charging demand-supply relationship based on the assumptions outlined in Section 2.2. For zones without charging stations, we connect them to their nearest station (i.e., $k = 1$ in Algorithm 1). The resulting network representation is shown in Figure 6, where red circle nodes represent service zone centroids and blue square nodes denote EV charging stations. The network contains 398 links with a weight of zero and 105 links with a weight greater than zero (indicating zones without charging stations, connected to nearby stations with driving distance as the link weight). In the network model, these 105 zones have a degree of 1 and are represented by weighted green dashed links in the plot. Geographically, most of these 105 zones are located in peripheral regions of the city. As the distance from the city center increases, EV drivers in these zones must travel longer to access charging resources in nearby regions. This highlights the uneven distribution of the charging infrastructure, particularly the severe scarcity of resources in rural areas.

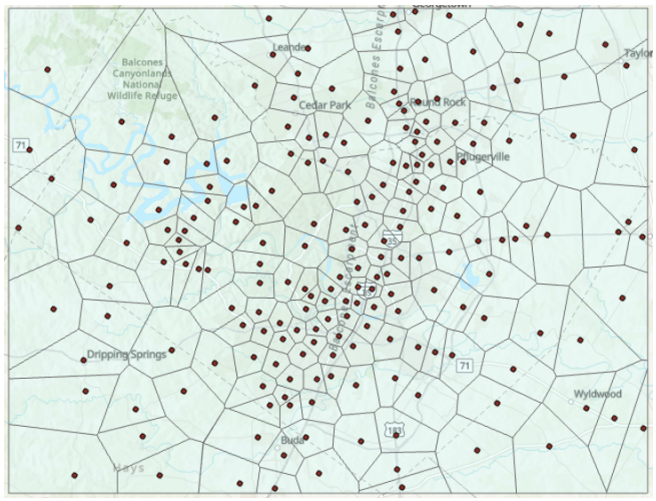

(a) Partitioned local service zones and their centroids, purely based on geographical locations of EV charging stations, POIs, and traffic cameras

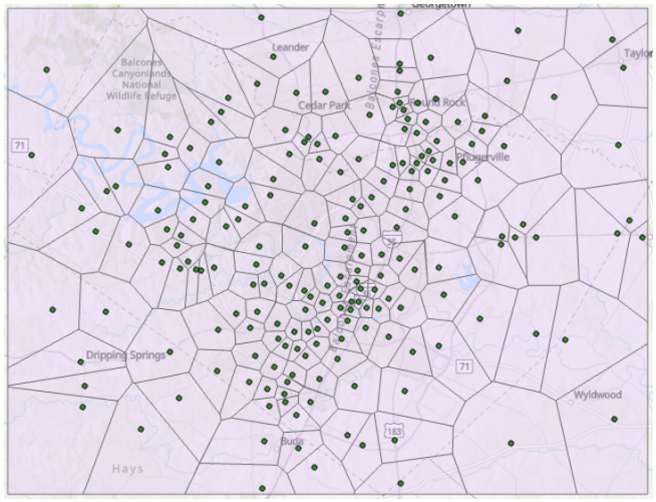

(b) Partitioned local service zones and their centroids, considering geographical locations of EV charging stations, POIs, and traffic cameras, and their varied contributions to charging demand

FIGURE 5: Partitioned service zones.

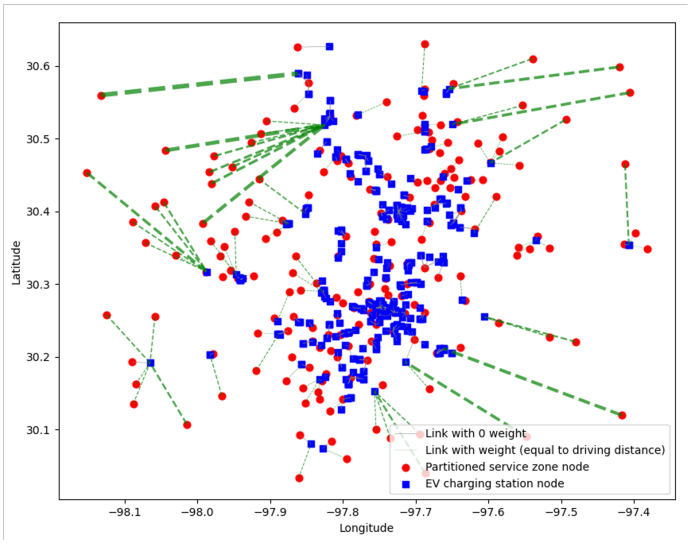

FIGURE 6: Bipartite network representation of charging demand-resources alignment in Austin area.

3.4 PUBLIC EV CHARGING SYSTEM OPTIMIZATION

3.4.1 The scheme of test cases In this section, we follow the methodology outlined in Section 2.3 to formulate and solve the optimization problem for optimal planning of the public EV charging infrastructure in the Austin area, ensuring that newly planned resources can support the projected increase in daily charging demand for the next year. We begin by clarifying several assumptions. First, we use the recorded total number of charged EVs at existing stations in a single day (10,731) to represent the current year's daily charging demand, evenly distributed across local service zones (approximately 54 EVs per zone). Next, we calculate the average growth rate of registered EVs in the Austin area from 2017 to 2024, which is 175.73%. Based on this, the projected daily charging demand for the next year is approximately 149 EVs per zone. Second, since the charging capacity b_i of each station is critical for calculating both driving costs and coverage efficiency, we develop a regression model to estimate the number of EVs a station can charge daily based on its total charger power. The results, provided in Table 4, indicate that a Level 2 charger with 6.6 kW of power can charge approximately 4 cars per day. Third, the power constraint for this study is set at 4000 kW, corresponding to the maximum total power observed among existing EV charging stations. However, real-world grid constraints vary by location, and future work will incorporate transformer capacity data for a more accurate representation. Finally, to explore the impact of different design configurations, we examine three test cases, as summarized in Table 5. These cases vary in terms of budget constraints and charger types, enabling us to evaluate the trade-offs and effectiveness of various planning approaches under realistic conditions.

3.4.2 Setup for solving the test cases In this case study, we consider 398 existing charging stations and 105 zones without charging stations, using the centroids of these zones as candidate locations for new stations. Due to computational resource limitations, we restrict each test case to a single charger type. Consequently, the design variable vector $\mathbf{Q}$ has a length of 503 for all test cases. Additionally, we impose a constraint limiting the total number of chargers installed across existing and new stations to 10 for each charger type. For the genetic algorithm (GA) hyperparameters, we set the population size to 50,

TABLE 4: Regression results: the relation between the sum of EV charger powers in a station and the number of EVs that station can charge in a day[1]

	Coef	Std err	t	$p > \|t\|$
Const	3.5845	0.093	38.512	< 0.001
Avg traffic flow	0.0187	0.001	18.644	< 0.0001

[1]: The model achieves an R-squared value of 0.43, indicating moderate explanatory power but limited accuracy in predicting the number of charged EVs based on power support. In future work, we will explore more advanced modeling techniques and incorporate additional data sources to enhance the model's predictive performance.

TABLE 5: Scheme of test cases

Test case	Budget ($)[1]	Charger type
Case One	1 Billion	Level 2 (6.6 kW)
Case Two	1 Billion	DC 50 kW
Case Three	0.1 Billion	DC 50 kW

[1]: In future work, we will consider DC 150 kW and DC 350 kW chargers as additional options. The $1 billion budget estimate is based on a value higher than the cost of installing ten DC 350 kW chargers across all 503 existing and candidate stations (approximately $0.8 billion). Similarly, the $0.1 billion estimate is derived from a value lower than the cost of installing ten DC 50 kW chargers across all stations (approximately $0.2 billion).

the mutation rate to 15% per generation, the maximum number of generations to 100, and the stopping criterion to 20 consecutive generations without improvement in the best objective value (fitness).

3.4.3 Results The computation processes for Test Cases One, Two, and Three terminate at 52, 72, and 100 generations, respectively, each exhibiting an evident converging trend. The resulting placements of new chargers for both station expansions and new station establishments are illustrated in Figure 7 (a)∼(c). Comparing the three layouts reveals that, given sufficient budget, Test Cases One and Two feature numerous large orange circles and blue triangles distributed across the region, indicating extensive expansion of existing stations and installation of new stations. Statistically, 87% and 84% of existing stations are expanded, while 97% and 96% of candidate stations are constructed in Test Cases One and Two, respectively. The key differences between Test Cases One and Two include: (1) Test Case One prioritizes expansion of stations in the downtown area, as evidenced by the higher density of large orange circles within the red circle in Figure 7a compared to Figure 7b; and (2) Test Case One establishes new large-sized stations more evenly throughout the region, while Test Case Two shows a more clustered distribution of large-sized new stations in the northern region, highlighted by the red square in Figure 7b. In contrast, Test Case Three, with a significantly smaller budget, focuses more on expanding existing stations rather than establishing new ones. This results in an 83% expansion rate, comparable to Test Case Two, and an 83% establishment rate for new stations. However, the scale of expansion in Test Case Three is smaller than in the other two cases, as highlighted by the red square in Figure 7c, reflecting the constraints imposed by its limited budget.

In Figure 7 (e)∼(g), we present the bipartite network representations based on the placements of the three test cases. These plots clearly visualize the alignment between charging demand and resources. Both Test Case One and Two establish a sufficient number of new charging stations to cover the majority of rural regions' charging demand, as indicated by the limited number of green links. However, they overlook a few remote rural regions, evidenced by the thick green links in the upper left of Test Case One's plot and the lower right of Test Case Two's plot. In contrast, Test Case Three demonstrates a lower coverage ratio for rural region charging demand, but establishes new stations more evenly across rural areas, resulting in more green links with smaller weights.

Finally, we compare the total expenses, unmet charging demand, and driving costs across the three test cases. Test Case One invests a moderate amount (approximately $12 million) but serves the fewest EVs, leaving about 26,000 EVs' charging demand unmet (approximately 88% of the total daily demand). This suggests that Level 2 chargers, even with moderate investment, are insufficient to fully meet the region's needs. In contrast, Test Case Two spends around $104 million, meeting 4% more charging demand than Case One and significantly reducing the total driving distance to about 53,000 km, which is 34% of Test Case One and 15% of Test Case Three. Test Case Three, with less funding, invests nearly $95 million and meets 3% more demand than Case One. However, its relatively sparse station deployment results in significantly longer driving distances, highlighting the trade-offs imposed by a limited budget on charger placement and coverage.

4 LIMITATION

This work has four key limitations, which are illustrated as below:

1) The first limitation of this study is the exclusion of temporal effects in the research framework. Time factors could significantly influence several aspects of the analysis. First, different types of locations may affect the dwelling time of EV drivers, thereby influencing charging duration. Incorpo-

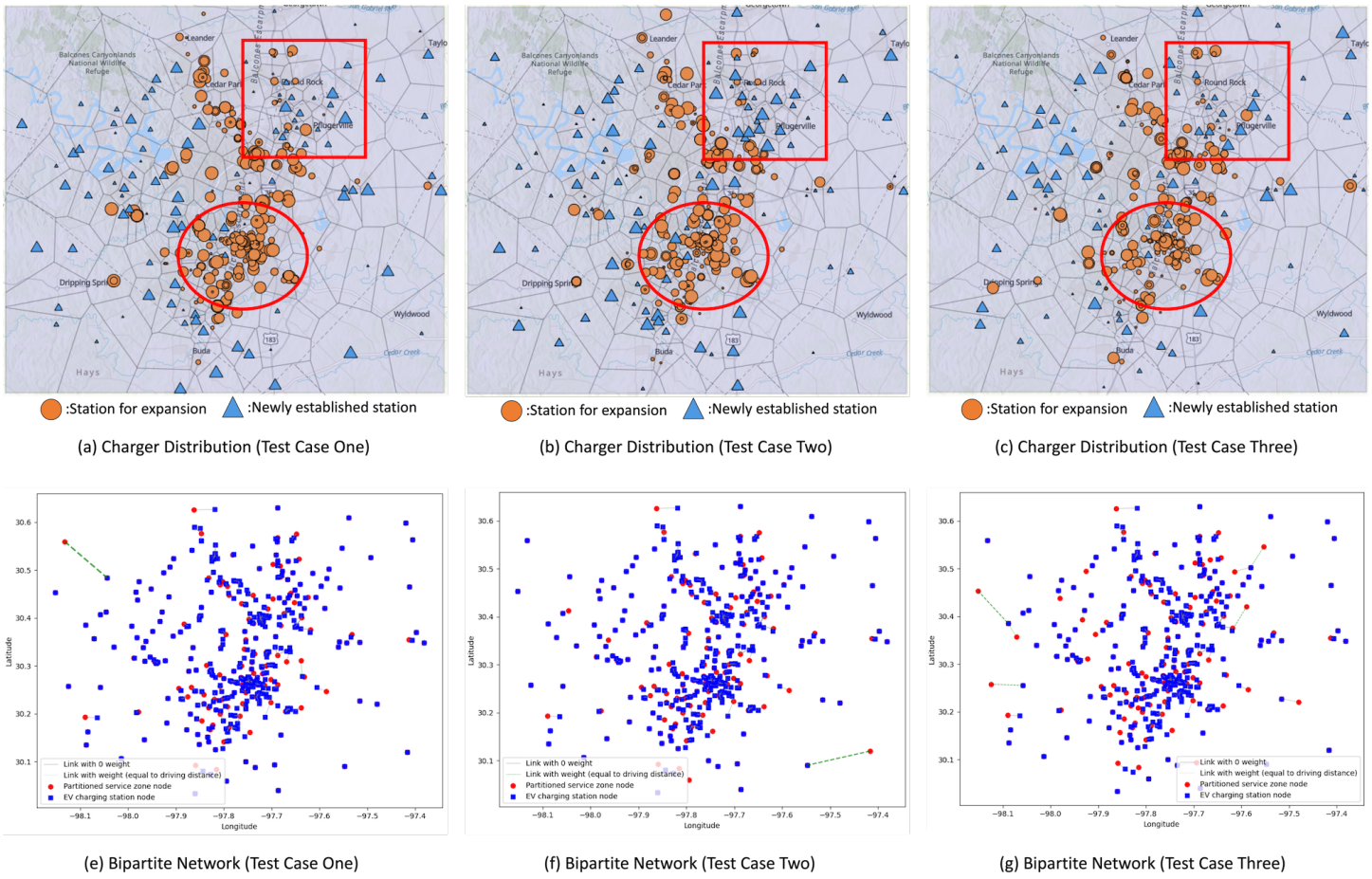

(a) Charger Distribution (Test Case One)

(b) Charger Distribution (Test Case Two)

(c) Charger Distribution (Test Case Three)

(e) Bipartite Network (Test Case One)

(f) Bipartite Network (Test Case Two)

(g) Bipartite Network (Test Case Three)

FIGURE 7: Optimal EV charger placements and bipartite network representations for the three test cases. Test Case One focuses on expanding Level 2 (6.6 kW) chargers with a high budget, Test Case Two prioritizes DC 50 kW fast chargers for regional coverage with a sufficient budget, and Test Case Three optimizes DC 50 kW charger placement under a limited budget. Larger shapes on the map indicate a higher number of installed chargers.

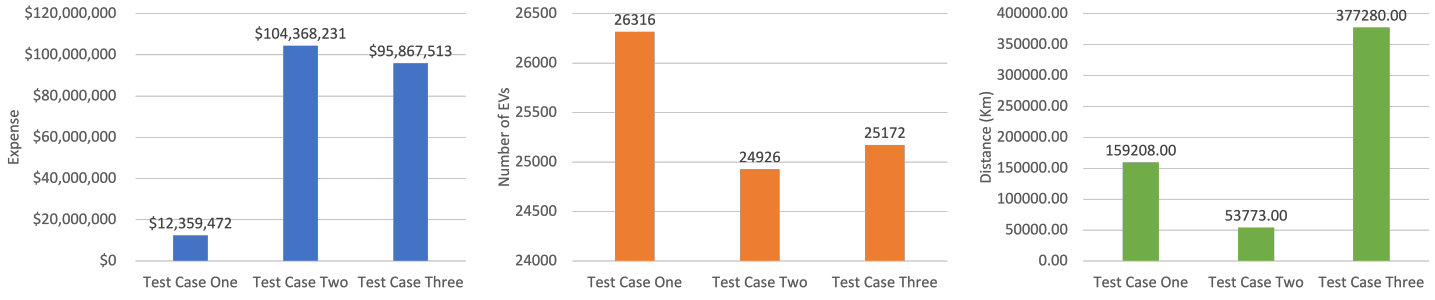

(a) Total Expenses

(b) Unmet Charging Demand

(c) Driving Cost

FIGURE 8: Comparison of objective function values across three test cases.

rating temporal considerations could improve the accuracy of local service zone partitioning. Second, in calculating coverage efficiency, we aggregate daily charging records to estimate the relationship between the number of charged ve-

hicles and a station's total power capacity. However, ignoring the differing charging speeds of Level 2 and fast chargers may underestimate the higher demand coverage efficiency of fast chargers. Addressing these temporal factors is essential for more accurate modeling and analysis.

2) The second limitation is that, as the first study to adopt a choice modeling philosophy to model the alignment between local charging demand and resources using a bipartite network, we still lack a deep understanding of the network structure. For instance, it remains unclear which charging resource allocation strategies or specific local network structures (e.g., building a supercharging station to connect with many service zones or building small-scale charging stations to connect with a few service zones) are most beneficial for optimizing the overall charging system. This limits the exploitation of the bipartite network model with more advanced network modeling techniques, such as graph neural networks [25, 26] and multidimensional network analysis [27, 28]. Further advanced studies are necessary to fully uncover the unique potential of this bipartite network-based framework and its ability to guide the optimal design of EV charging systems.
3) As outlined in Section 2.3, this study assumes a fixed power limitation for each station. However, in practice, different connection points in the power grid across the city may have varying power capacities. Incorporating these variations is critical to ensuring both the reliable operation of charging stations and the stability of the power grid.
4) Another key limitation of this study is the low computational efficiency in solving the optimization problem. The experiments were conducted on a computer equipped with an 11th-generation Intel Core CPU (i9-11900, 2.50 GHz, 8 cores, 16 logical processors) and 32 GB of RAM. Using a parallel computing strategy with 12 logical processors, the computational time for 100 generations was approximately 50 hours. This inefficiency is largely due to the high dimensionality of the design space, $\mathbf{Q}$. A potential solution is to reformulate the optimization problem as a sequential decision-making process: first determining which existing stations to expand and where to build new stations, followed by optimizing the number of chargers to install. In future work, we will explore this approach and advanced parallel computing algorithms tailored for high-dimensional optimization problems.

5 CONCLUSION

The study introduces a novel framework for optimizing the placement and allocation of EV charging infrastructure, addressing the limitations of traditional grid-based methods that fail to account for spillover effects between sub-regions. By integrating Voronoi diagrams with weighted K-means clustering, our approach partitions regions based on spatially relevant factors such as POIs and traffic flow, ensuring a more accurate representation of local charging demand. Additionally, the use of a bipartite network model, grounded in choice modeling principles, captures the alignment between charging demand and resources, enabling an integrated approach to infrastructure planning. The framework's effectiveness is demonstrated through a case study in Austin, Texas. We optimize charging resource allocation by expanding existing stations, selecting new locations, and determining charger types and quantities while minimizing driving costs and total expenses within budget and power constraints.

We examine three test cases, varying in budget and charger types. The results highlight the framework's ability to balance spatial equity and demand-driven allocation. Test Case One (Level 2, 6.6 kW chargers) and Test Case Two (DC 50 kW chargers), with sufficient budgets, achieve extensive coverage in urban areas. In contrast, Test Case Three (DC 50 kW chargers), with limited funding, focuses more on expanding existing stations rather than establishing new ones, revealing trade-offs in resource allocation. Bipartite network visualizations underscore the importance of addressing rural demand gaps and optimizing station placement to reduce driving distances. Beyond EV charging, the framework's flexibility suggests potential applicability to other facility allocation and policy design problems, such as public transportation hubs or renewable energy infrastructure, where user demand and resource dependencies are critical.

In future work, we will mainly focus on five key directions: 1) incorporating temporal factors, such as variations in charging behavior and speed differences between Level 2 and fast chargers, to improve demand prediction and resource allocation efficiency; 2) exploring the characteristics of the bipartite network model to fully uncover its potential to guide the optimal design of EV charging infrastructure; 3) integrating real-world power grid constraints to enhance system reliability and stability; 4) conducting sensitivity analysis for different configurations of the proposed framework, such as evaluating how the number of partitioned service zones affects optimization outcomes, will provide valuable insights into the robustness and scalability of the approach; 5) developing more efficient algorithms and parallel computing techniques to address high-dimensional optimization challenges. These efforts will refine the framework and expand its applicability to EV charging infrastructure and other facility allocation problems.

REFERENCES

[1] Bouckaert, S., Pales, A. F., McGlade, C., Remme, U., Wanner, B., Varro, L., D'Ambrosio, D., and Spencer, T., 2021. Net zero by 2050: A roadmap for the global energy sector. Tech. rep., The International Energy Agency (IEA).

[2] Wood, E., Borlaug, B., Moniot, M., Lee, D.-Y. D., Ge, Y., Yang, F., and Liu, Z., 2023. The 2030 national charging network: Estimating us light-duty demand for electric vehi-

cle charging infrastructure. Tech. rep., National Renewable Energy Laboratory (NREL), Golden, CO (United States).

[3] Laboratory, A. N., 2025. Light duty electric drive vehicles monthly sales updates. Last accessed 10 March 2025.

[4] Brown, A., Cappellucci, J., Heinrich, A., Gaus, M., and Cost, E., 2024. Electric vehicle charging infrastructure trends from the alternative fueling station locator: First quarter 2024. Tech. rep., National Renewable Energy Laboratory (NREL), Golden, CO (United States).

[5] Yi, Z., Liu, X. C., Wei, R., Chen, X., and Dai, J., 2022. "Electric vehicle charging demand forecasting using deep learning model". *Journal of Intelligent Transportation Systems,* ***26***(6), pp. 690–703.

[6] Wang, S., Chen, A., Wang, P., and Zhuge, C., 2023. "Predicting electric vehicle charging demand using a heterogeneous spatio-temporal graph convolutional network". *Transportation Research Part C: Emerging Technologies,* ***153***, p. 104205.

[7] Shahraki, N., Cai, H., Turkay, M., and Xu, M., 2015. "Optimal locations of electric public charging stations using real world vehicle travel patterns". *Transportation Research Part D: Transport and Environment,* ***41***, pp. 165–176.

[8] Liang, Y., Wang, H., and Zhao, X., 2022. "Analysis of factors affecting economic operation of electric vehicle charging station based on dematel-ism". *Computers & Industrial Engineering,* ***163***, p. 107818.

[9] Nicholas, M., 2019. "Estimating electric vehicle charging infrastructure costs across major us metropolitan areas". ICCT Washington, DC, USA.

[10] Li, Y., and Jenn, A., 2024. "Impact of electric vehicle charging demand on power distribution grid congestion". *Proceedings of the National Academy of Sciences,* ***121***(18), p. e2317599121.

[11] Acharige, S. S., Haque, M. E., Arif, M. T., Hosseinzadeh, N., Hasan, K. N., and Oo, A. M. T., 2023. "Review of electric vehicle charging technologies, standards, architectures, and converter configurations". *IEEE access,* ***11***, pp. 41218–41255.

[12] Greaker, M., 2021. "Optimal regulatory policies for charging of electric vehicles". *Transportation Research Part D: Transport and Environment,* ***97***, p. 102922.

[13] Anadón Martínez, V., and Sumper, A., 2023. "Planning and operation objectives of public electric vehicle charging infrastructures: A review". *Energies,* ***16***(14), p. 5431.

[14] Ullah, I., Zheng, J., Jamal, A., Zahid, M., Almoshageh, M., and Safdar, M., 2024. "Electric vehicles charging infrastructure planning: a review". *International Journal of Green Energy,* ***21***(7), pp. 1710–1728.

[15] Prakobkaew, P., and Sirisumrannukul, S., 2024. "Optimal locating and sizing of charging stations for large-scale areas based on gis data and grid partitioning". *IET Generation, Transmission & Distribution,* ***18***(6), pp. 1235–1254.

[16] Aurenhammer, F., 1991. "Voronoi diagrams—a survey of a fundamental geometric data structure". *ACM Comput. Surv.,* ***23***(3), Sept., p. 345–405.

[17] Modha, D. S., and Spangler, W. S., 2003. "Feature weighting in k-means clustering". *Machine learning,* ***52***, pp. 217–237.

[18] Ben-Akiva, M., McFadden, D., Train, K., Walker, J., Bhat, C., Bierlaire, M., Bolduc, D., Boersch-Supan, A., Brownstone, D., Bunch, D. S., et al., 2002. "Hybrid choice models: Progress and challenges". *Marketing Letters,* ***13***, pp. 163–175.

[19] Sha, Z., Cui, Y., Xiao, Y., Stathopoulos, A., Contractor, N., Fu, Y., and Chen, W., 2023. "A network-based discrete choice model for decision-based design". *Design Science,* ***9***, p. e7.

[20] Hartigan, J. A., and Wong, M. A., 1979. "Algorithm as 136: A k-means clustering algorithm". *Journal of the royal statistical society. series c (applied statistics),* ***28***(1), pp. 100–108.

[21] Pagany, R., Marquardt, A., and Zink, R., 2019. "Electric charging demand location model—a user-and destination-based locating approach for electric vehicle charging stations". *Sustainability,* ***11***(8), p. 2301.

[22] Kavianipour, M., Fakhrmoosavi, F., Singh, H., Ghamami, M., Zockaie, A., Ouyang, Y., and Jackson, R., 2021. "Electric vehicle fast charging infrastructure planning in urban networks considering daily travel and charging behavior". *Transportation Research Part D: Transport and Environment,* ***93***, p. 102769.

[23] Dijkstra, E. W., 2022. "A note on two problems in connexion with graphs". In *Edsger Wybe Dijkstra: his life, work, and legacy*. pp. 287–290.

[24] Mitchell, M., 1998. *An introduction to genetic algorithms*. MIT press.

[25] Xiao, Y., Ahmed, F., and Sha, Z., 2023. "Graph neural network-based design decision support for shared mobility systems". *Journal of Mechanical Design,* ***145***(9), p. 091703.

[26] Zhang, C., Song, D., Huang, C., Swami, A., and Chawla, N. V., 2019. "Heterogeneous graph neural network". In Proceedings of the 25th ACM SIGKDD international conference on knowledge discovery & data mining, pp. 793–803.

[27] Wang, M., Chen, W., Huang, Y., Contractor, N. S., and Fu, Y., 2016. "Modeling customer preferences using multidimensional network analysis in engineering design". *Design Science,* ***2***, p. e11.

[28] Cui, Y., Sun, Z., Xiao, Y., Sha, Z., Koskinen, J., Contractor, N., and Chen, W., 2024. "Network analysis of two-stage customer decisions with preference-guided market segmentation". *Journal of Computing and Information Science in Engineering*, 09, pp. 1–28.